EXPERIMENTAL AND NUMERICAL INVESTIGATIONS ON THE PERFORMANCE OF FLEXIBLE SKIN FLAPPING WING FOR MICRO AERIAL VEHICLE APPLICATION

HAMID YUSOFF

UNIVERSITI SAINS MALAYSIA

2013

EXPERIMENTAL AND NUMERICAL INVESTIGATIONS ON THE PERFORMANCE OF FLEXIBLE SKIN FLAPPING WING FOR MICRO AERIAL VEHICLE APPLICATION

by

HAMID YUSOFF

Thesis submitted in fulfilment of the requirements

for the degree of

Doctor of Philosophy

JULY 2013

DECLARATION

I hereby declare that the work reported in this thesis is the result of my own investigation and that no part of the thesis has been plagiarized from external sources. Materials taken from other sources are duly acknowledged by giving explicit references.

Signature: ……..

Name of student: HAMID YUSOFF

Matrix number: P-CD 0052

Date: 16 July 2013

ACKNOWLEDGEMENTS

“In the name of ALLAH, The Most Beneficent and The Most Merciful”

All praises to Allah S.W.T, the most merciful and gracious, and my peace and blessings of Allah be upon his messenger, Muhammad S.A.W. First of all, I would like to express my gratitude to his greatness, with whose indulgence has given me the strength and convenience to complete this report successfully.

I would like to express my sincere appreciation and admiration to my advisors, Prof. Dr. Mohd Zulkifly Abdullah and Dr Kamarul Arifin, for their continuous support, guidance and hard work. Both of them are friendship, have an optimistic attitude, always brightened any experimental challenge and provided that extra boost to keep forging ahead. Many thanks also go to all my lecturers in the School of Mechanical Engineering who have given me a firm background in fluid mechanic, which assisted me in many ways throughout my postgraduate study. I also would like to extend my appreciation to other committee members, Khalil, Fairuz, Ahsraf, Kamal, Zubir and Mujeebu for their friendship, and talents to aid in their success of my research goals.

I also would like to thank the technical staffs of the School of Mechanical Engineering, who have assisted me in one way or another, towards the success of this project. Many thanks are accorded to Mr. Najhan, Mr. Zaimi, Mr. Norijas, Mr. Komarudin, Mr Hashim, Mr. Zalmi, Mr Faris and others for their co-operation in laboratory works.

Without a doubt, my family members have been the largest supporters throughout my academic career. I must say a special ‘thank you’ to my parents,

Yusoff and Hasmah, and for all my brother and sister for their continuous love and words of encouragement. The successes I have achieved did not come without certain sacrifices, which they all endured in some form. I am ever grateful for my best friend for Erham and Asrul encouragement and his motivate since the first day we met. Also many thanks to all other parties that I have not mentioned their names here, whose have helped me directly or indirectly throughout my study. May Allah S.W.T bless all of you.

Finally, I am grateful to the Universiti Sains Malaysia for giving opportunity for this postgraduate study.Praise is exclusively to Allah. The Lord of the universe and Peace is upon the Master of the Messengers, his family and companions.

Hamid Yusoff

July 2013

TABLE OF CONTENTS

	PAGE
ACKNOWLEDGEMENTS	ii
TABLE OF CONTENTS	iv
LIST OF TABLES	x
LIST OF FIGURES	xii
LIST OF SYMBOLS	xix
LIST OF ABBREVIATION	xxi
ABSTRAK	xxiv
ABSTRACT	xxvi
CHAPTER 1: INTRODUCTION	1
1.1 Micro Air Vehicles (MAVs)	1
1.2 Application of MAVs	3
1.3 Biologically of MAV designs	6
1.4 Problem statement	10
1.5 Contribution of the present research	11
1.6 Objective of the research	13
1.7 Scope of the research	14
1.8 Thesis outline	15
CHAPTER 2: LITERATURE REVIEW	16
2.1 Overview	16
2.2 Development of FW-MAV	16
2.3 Aerodynamic mechanism of flapping wing	23
2.3.1 Wagner Effect	23
2.3.2 Leading edge vortex	25

2.3.3 Clap and cling mechanism 26

2.3.4 Rotational lift 27

2.3.5 Wing-wake interactions 28

2.3.6 Lift force 29

2.4 Aerodynamic design requirements for FW-MAV 31

2.4.1 Wing flexibility study 31

2.4.2 Adaptive flow control techniques 35

2.4.3 Wing shape plan form characterization 36

2.5 Optimization enhancement an aerodynamic of FW-MAV 41

2.6 Concluding remarks 45

CHAPTER 3: FLAPPER DESIGN 48

3.1 Wing Development 48

3.1.1 Obtaining wing design specification of bat wing 48

3.1.2 Fabrication of wing frame and membrane 50

3.2 Flapper Mechanism 52

3.2.1 Four-bar linkage mechanism 52

3.2.2 Kinematics of Four-bar linkage mechanism 55

3.3 Electronic Control System 57

3.3.1 System Architecture Overview 57

3.3.2 PIC16F876 Microcontroller 59

3.3.3 Electronic System Flow 62

3.3.4 ECS testing Procedure 64

CHAPTER 4: METHODOLOGY 67

4.1 Overview 67

4.1 Experimental setup and procedure 67

4.1.1	Test facilities		67
	4.1.1.1	Air chamber	67
	4.1.1.2	Force measurement systems	67
4.1.2	Wing model		68
	4.1.2.1	Flexible membrane skin	69
	4.1.2.2	Cambered wing	71
4.1.3	Testing Procedure		72
4.1.4	Dimensionless parameters		76
4.1.5	Filter data		77
4.1.6	Inertial force measurement		79
4.1.7	Error analysis		83
	4.1.7.1	Types of Experimental Errors	83
	4.1.7.2	Mean, Standard Deviation and Standard Error	84
4.1.8	Uncertainty analysis		85
	4.1.8.1	Force balance uncertainty	86
	4.1.8.2	Uncertainty for instantaneous lift and drag	87
	4.1.8.3	Uncertainty for time averaged lift and drag coefficient	88
4.1.9	Design of experiment (DOE)		89
	4.1.9.1	Introduction	89
	4.1.9.2	Performance characteristics	91
	4.1.9.3	Experimental conditions and plan	91
4.2	Numerical setup and procedure		93

4.2.1 Computational model 93
4.2.2 Time step-dependency solution 95
4.2.3 Mesh-dependency solution 97
4.2.4 Governing equation 99
4.2.5 Prescribed mesh motion and mesh updates 101
4.2.6 Simulation procedure 102
CHAPTER 5: RESULTS AND DISCUSSION 105
5.1 Overview 105
5.2 Flapper performances 105
5.2.1 Flapping angle, angular velocity and acceleration 105
5.2.2 ECS performances 108
5.3 Flexibility study 110
5.3.1 Effect of skin flexibility as functions of f and Re 110
5.3.2 Comparison of flexibility at low and high Re 121
5.3.3 Effect of Skin flexibility as functions of AoA 126
5.3.4 Effect of skin flexibility as function of J 131
5.4 Camber and optimization study 135
5.4.1 Effect of camber as functions of f and Re 135
5.4.2 Comparison of lifts and drag performance based on varying wing camber at low Re 142
5.4.3 Unsteady effect of lift and drag performance 144
5.4.4 Effect of camber wing as functions of AoA and Re 145
5.4.5 Design of Experiments (DOE) 155
5.4.5.1 Analysis of Variance (ANOVA) 156

5.4.5.2 Effect of design parameters on the ε_{aero} 159
5.4.5.3 Optimization of design parameters 162
5.4.5.4 Confirmation experiments 162
5.5 CFD results and discussion 163
5.5.1 Comparison of simulation and experiment 163
5.5.1.1 Similarities in the quantitative of time averaged lift and drag force for dimensionless of advance ratio 163
5.5.1.2 Similarities in the time histories of lift and drag force 164
5.5.1.3 Verification of the unsteady effect 168
5.6.1.3.1 Unsteady lift force during down stroke 168
5.6.1.3.2 Unsteady lift force during up stroke 169
5.5.1.4 Evaluation of aerodynamic force based on maintenance of LEV 172
5.5.1.5 Effect of the camber wing on the performance of aerodynamic 176
5.5.1.6 LEV improves lift by influence of camber 180
CHAPTER 6: CONCLUSIONS AND FUTURE WORK 185
6.1 Conclusions 185
6.1.1 Experimental characterization 185
6.1.2 Numerical characterization 187

6.2 Suggestions for future work 188

REFERENCES 189

APPENDICES 189

LIST OF PUBLICATIONS 219

LIST OF TABLES

NO	TABLES	PAGE
1.1	MAVs with mission specification and applications	6
1.2	MAV characteristic	6
2.1	Flapping mechanism based on experimental setup	23
2.2	Types of wing flexibility	34
2.3	Several of wing shape plan form study reported from previous authors	40
2.4	List of optimization methods and parameters study on flapping wing	45
3.1	Wing bat parameters of three species and present study	49
3.2	Flight parameters of three species and present study	50
3.3	Analog voltage to 8-bit of PIC microcontroller's ADC	61
4.1	Specifications of the test wings	70
4.2	The series of wings model geometry	71
4.3	The parameters and variable of test conditions for flexible wings (wing A,B and C)	73
4.4	The parameters and variable of test conditions for camber wings (0, 6, 9, 12, and 15%)	73
4.5	Show the mean inertial force distribution at Wing C at AoA 10^0 and velocity 7 ms^{-1} at various frequencies.	82
4.6	Error analysis for force balance on lift calibration factor	86
4.7	Error analysis for force balance on drag calibration factor	86
4.8	Uncertainty error for instantaneous C_D for 10 cycles	87
4.9	Uncertainty error for instantaneous C_L for 10 cycles	88
4.10	Lift error for time average force coefficient	89
4.11	Drag error for time average force coefficient	89

4.12	Independent variables of the CCD design	92
4.13	Time step size for time-dependency solution	96
4.14	Details of mesh dependency solution in flow solver	98
5.1	Comparison of $C_{L\,avg}$ based on flexibility condition at low and high Re. (F = 9 Hz, AoA =10^0)	125
5.2	Comparison of $C_{D\,avg}$ based on flexibility condition at low and high Re. (F = 9 Hz, AoA =100)	125
5.3	Comparison of lift slope	131
5.4	Enhancement of $C_{L\,avg}$ based on camber condition at Re = 3600 (F = 9 Hz, AoA =10^0)	144
5.5	Enhancement of $C_{D\,avg}$ based on camber condition at Re = 3600 (F = 9 Hz, AoA =10^0)	144
5.6	Enhancement of $C_{L\,avg}$ based on camber condition at Re = 3600 (F = 9 Hz, AoA =10^0)	155
5.7	Design of experimental matrix and results for the ε_{aero} characteristics	196
5.8	ANOVA table for the ε_{aero} (before elimination)	157
5.9	ANOVA table for the ε_{aero} (after elimination)	158
5.10	Optimization results for aerodynamic efficiency (ε_{aero})	162
5.11	Confirmation experiment	163
5.12	CFD test condition	170

LIST OF FIGURES

NO	FIGURES	PAGE
1.1	MAV flight regime compared to existing flight vehicles.Pornsin-sirirak et al., (2001).	3
1.2	Types of Fix-wing, rotary-wing and flapping wing MAVs	4
1.3	a) Sugar glider by Galvao et al., (2006), b) the large degree of camber in the wing. The unique aerodynamic properties of a compliant-membrane wing are believed to play a significant role in the high degree of maneuverability exhibited by bats in flight by Song et al., (2008).	7
2.1	Three generation of Microbat prototypes developed by Pornsin-sirirak et al., (2000).	17
2.2	a) Passive by Pornsin-sirirak et al., (2002) and b) active by Liger et al., (2002) adaptive of flow control actuator intended onto MEMs wing.	18
2.3	Propelled by a pair of wing symmetry produced by Jones et al., (2004).	19
2.4	Wagner effect. The ratio of instantaneous to steady circulation (*y*-axis) grows as the trailing edge vortex moves away from the airfoil (inset), and its influence on the circulation around the airfoil diminishes with distance (*x*-axis) by Sane, (2003).	24
2.5	Leading edge vortex on the wing by Sane, (2003).	26
2.6	Evolution of a leading edge vortex in (A) two dimensions and (B) three dimensions during linear translation starting from rest Sane, (2003).	26
2.7	Schematic representation of the clap (A-C) and ing (D-F) Sane, (2003).	27
2.8	Three phases of the wing rotation Dickinson, (1994).	28
2.9	Wing-wake interaction during stroke reversal Sane, (2003).	29
2.10	Flight forces for the drosophila during hovering Fry et al., (2005).	30
2.11	Schematic of the alula acting on the leading edge wing Meseguer et al., (2005).	36

3.1	Plot of the wing span vs. total weight Bullen, (2002).	49
3.2	The wing construction and photograph of bat wing skin. a)Wing construction and b) Natural wing produce by Norberg, (2006).	51
3.3	The combined of slider rod mechanism and movable hinge. Left figure show and isometric view and right figure front view of mechanism.	53
3.4	Working sequence of flapper design.	53
3.5	Assembly of flapping wing system (not to scale).	54
3.6	The kinematic model of the flapping mechanism.	57
3.7	The control system block diagram.	59
3.8	The control system prototype board.	59
3.9	PWM waveforms of two different duty cycles.	60
3.10	8N1 configuration; 8 data bits, no parity bit and 1 stop bit.	60
3.11	The variable resistor pins connection.	61
3.12	Flow Chart of the ECS executed system.	63
3.13	a) Schematic of experiment setup of flapping mechanism using Electronic Control System and Load-cell for calibration and comparing. b) The photo showed the experiment apparatus and measurement devices.	66
4.1	a) Front view open test section; b) rear view and c) schematic of air chamber with test stand setup.	68
4.2	Four beam strain gauge balance.	69
4.3	Kyowa PCD-300A sensor interface.	69
4.4	The test wings (A-least flexible, B-flexible and C-most flexible).	70
4.5	Schematic of a) flat wing thickness and b) Photo of side view of flat wing. Schematic of c) camber wing show configuration of height of camber wing respect to chord length and d) Photo of side view of camber wing.	71
4.6	a) The photo of experimental setup in the left and b) large view of flapping mechanism in the right figure.	74

4.7	The flow of lift and drag measurement.	75
4.8	Raw data at flapping frequency 9 Hz, AoA 10 degree, and velocity V = 7.0 m/s.	79
4.9	Filtered data at flapping frequency 9 Hz, AoA 10 degree, and velocity V = 7.0 m/s.	79
4.10	Uncovered wing for inertial force testing.	81
4.11	Inertial force for uncovered wing. (9 Hz flapping frequency at AoA 10^0 and Velocity 7 ms^{-1} for Wing C.	82
4.12	Uncertainty Curve for 1 m/s, 9 Hz, 10^0 AoA with Wing C for 10 cycles.	88
4.13	Simulation models; the FLUENT meshed model showing boundary conditions and computational domain.	95
4.14	Time-dependency solution; Lift coefficient, C_L vs. time dimensionless t/T.	96
4.15	Time-dependency solution; Drag coefficient, C_D vs. time dimensionless t/T.	96
4.16	Mesh-dependency solution; Lift coefficient, C_L vs. time dimensionless.	98
4.17	Mesh-dependency solution; Drag coefficient, C_D vs. time dimensionless.	98
4.18	Steps in CFD analysis.	104
5.1	A sequence images of the wing for one cycle of flapping.	106
5.2	Flapping angle observed by high speed camera.	107
5.3	Comparison of experimental and theoretical flapping angle.	107
5.4	Figure 5.4: a) Variation of angular velocity and b) angular acceleration with crank angle.	108
5.5	Percentage of error in frequency distribution a) without ECS and b) with ECS.	109
5.6	$C_{L\ avg}$ vs. Reynolds number for various flapping frequencies at AoA 10^0 for Wing A.	112

5.7 $C_{L\ avg}$ vs. Reynolds number for various flapping frequencies at AoA 10^0 for Wing B. 113

5.8 $C_{L\ avg}$ vs. Reynolds number for various flapping frequencies at AoA 10^0 for Wing C. 113

5.9 $C_{D\ avg}$ vs. Reynolds number for various flapping frequencies at AoA 10^0 for Wing A. 114

5.10 $C_{D\ avg}$ vs. Reynolds number for various flapping frequencies at AoA 10^0 for Wing B. 114

5.11 $C_{D\ avg}$ vs. Reynolds number for various flapping frequencies at AoA 10^0 for Wing C. 115

5.12 $C_{L\ avg}$ vs. Reynolds number for various flexibilities at AoA 10^0 for 4Hz. 115

5.13 $C_{L\ avg}$ vs. Reynolds number for various flexibilities at AoA 10^0 for 5Hz. 116

5.14 $C_{L\ avg}$ vs. Reynolds number for various flexibilities at AoA 10^0 for 6Hz. 116

5.15 $C_{L\ avg}$ vs. Reynolds number for various flexibilities at AoA 10^0 for 7Hz. 117

5.16 $C_{L\ avg}$ vs. Reynolds number for various flexibilities at AoA 10^0 for 8Hz. 117

5.17 $C_{L\ avg}$ vs. Reynolds number for various flexibilities at AoA 10^0 for 9Hz. 118

5.18 $C_{D\ avg}$ vs. Reynolds number for various flexibilities at AoA 10^0 for 4Hz. 118

5.19 $C_{D\ avg}$ vs. Reynolds number for various flexibilities at AoA 10^0 for 5Hz. 119

5.20 $C_{D\ avg}$ vs. Reynolds number for various flexibilities at AoA 10^0 for 6Hz. 119

5.21 $C_{D\ avg}$ vs. Reynolds number for various flexibilities at AoA 10^0 for 7Hz. 120

5.22 $C_{D\ avg}$ vs. Reynolds number for various flexibilities at AoA 10^0 for 8Hz. 120

5.23 $C_{D\,avg}$ vs. Reynolds number for various flexibilities at AoA 10^0 for 9Hz. 121

5.24 Time averaged of lift coefficient from different configuration of flexibility at low and high Re for at flapping frequency 9Hz. (AoA 10^0). 124

5.25 Time averaged of drag coefficient from different configuration of flexibility at low and high Re for at flapping frequency 9Hz.(AoA 10^0). 125

5.26 $C_{L\,avg}$ vs. AoA for various flexibilities at V = 2 m/s (Reynolds number = 7200) for 9Hz. 129

5.27 $C_{L\,avg}$ vs. AoA for various flexibilities at V = 7 m/s (Reynolds number = 25200) for 9Hz. 129

5.28 $C_{D\,avg}$ vs. AoA for various flexibilities at V = 2 m/s (Reynolds number = 7200) for 9Hz. 130

5.29 $C_{D\,avg}$ vs. AoA for various flexibilities at V = 7 m/s (Reynolds number = 25200) for 9Hz. 130

.

5.30 $C_{L\,avg}$ vs. Advance ratio (J) for various flexibilities at AoA 10^0. 134

5.31 $C_{D\,avg}$ vs. Advance ratio (J) for various flexibilities at AoA 10^0. 135

5.32 $C_{L\,avg}$ vs. Reynolds number for various flapping frequencies at AoA 10^0. 138

5.33 $C_{D\,avg}$ vs. Reynolds number for various flapping frequencies at AoA 10^0. 139

5.34 $C_{L\,avg}$ vs. Reynolds number for various cambers at AoA 10^0. 140

5.35 $C_{D\,avg}$ vs. Reynolds number for various cambers at AoA 10^0. 141

5.36 Time averaged of lift coefficient from different configuration of camber at low and high Re for at flapping frequency 9Hz. (AoA 10^0). 143

5.37 Time averaged of drag coefficient from different configuration of camber at low and high Re for at flapping frequency 9Hz. (AoA 10^0). 143

5.38 $C_{L\,avg}$ respect to advance ratio (*J*). 146

5.39 $C_{D\,avg}$ respect to advance ratio (*J*). 146

5.40 C_L histories vs. t/T time dimensionless for various camber at flapping frequency of 9 Hz and AoA 10^0.(Re = 3600). 148

5.41 $C_{L\ avg}$ vs. AoA for various camber at (J = 0.88) for 9Hz. 151

5.42 $C_{L\ avg}$ vs. AoA for various camber at (J = 1.76) for 9Hz. 152

5.43 $C_{L\ avg}$ vs. AoA for various cambers at (J = 3.09) for 9Hz. 152

5.44 $C_{D\ avg}$ vs. AoA for various camber at (J = 0.88) for 9Hz. 153

5.45 $C_{D\ avg}$ vs. AoA for various cambers at (J = 1.76) for 9Hz. 153

5.46 $C_{D\ avg}$ vs. AoA for various cambers at (J = 3.09) for 9Hz. 154

5.47 Time averaged of lift coefficient maximum ($C_{L\ avg\ maximum}$) from different configuration of camber for advance ratio (i.e. J = 0.88, 1.76 and 3.09). The values of CL avg maximum were obtained at stall angle and flapping frequency at 9 Hz. 154

5.48 Normal probability plot of the studentized residual for $\varepsilon_{aero.}$ 159

5.49 Perturbation plot for aerodynamic efficiency (ε_{aero}) (Note: A = Camber, B = Velocity, and C = Frequency). 160

5.50 3D response surfaces for aerodynamic efficiency (ε_{aero}). 161

5.51 Comparison between experiment and simulation results of lift performances of a)flat, b) camber wing 6%, and c) camber wing 12%; $C_{L\ avg}$ vs. J at AoA 10^0. 165

5.52 Comparison between experiment and simulation results of drag performances of a)flat, b) camber wing 6%, and c) camber wing 12%; $C_{D\ avg}$ vs. J at AoA 10^0. 166

5.53 Lift coefficients histories at AoA 10^0, J = 0.44. (Flat wing). 167

5.54 Lift coefficients histories at AoA 10^0, J = 0.44. (Camber wing 6%). 167

5.55 Lift coefficients histories at AoA 10^0, J = 0.44. (Camber wing 12%). 167

5.56 Prescribed flapping motion for the Flat wing (normalized with respect to the time during one cycle). (Phase A, B, C, D and E representative time instants corresponding to T/t = 0, T/t =0.25, T/t =0.5, T/t = 0.75 and T/t =1, respectively, and are used at several places in this document for referencing purposes of down stroke and Upstroke case study of flow analysis. 170

5.57 Illustrated of test condition (phase and sheet a point of view). 170

5.58 Normalized path line averaged velocity according to the five time steps wing stroke location for one period flapping cycle beginning from down stroke to the up stroke location. 171

5.59 Flow pattern and pressure contours at three different time instant (phase A, B, and C as viewed from the down stroke frame moving with prescribed motion) around the flat wing at Z = 0.5b corresponding to sheet 3.(F = 1Hz, U = 1 m/s, J = 0.44 and AoA 10^0). 174

5.60 Flow pattern and pressure contours on the span (Z = 0.1b, 0.3b, 0.5b, 0.7b, and 0.9b) for time instants of Phase B in Figure 5.57). (F = 1Hz, U = 1 m/s, J = 0.44 and AoA 10^0). 175

5.61 Streamline (left) and span wise vorticity contour (right) at Z = 0.7b (Sheet 4) of the three tested wing at mid-down stroke (Phase b) and at J = 0.44. 178

5.62 Span wise pressure coefficient contour at Z = 0.7b (Sheet 4) of the three tested wing at mid-down stroke (Phase B) and at J = 0.44. 179

5.63 The non dimensional circulation, LEV radius, down wash velocity and lift coefficient of LEV along the wing span location. Results of the measurement from the flat wing at the mid down stroke (Phase B). The results indicated at the advance ratio J =0.44). 182

5.64 The non-dimensional circulation, LEV radius and down wash velocity for flat, camber 6%, and camber 12% at 0.7b wing semi span. The results indicated at the mid down stroke (Phase B) and the advance ratio J = 0.44 and AoA 10^0. 183

5.65 The C_{Lev} and % of enhancement for flat, camber 6%, and camber 12% at 0.7b wing semi span. The results indicated at the mid down stroke (Phase B) and the advance ratio J = 0.44. 184

LIST OF SYMBOLS

SYMBOL	DESCRIPTION	UNIT
English Symbols		
S_c	Motor speed constant	Rad/s
R_g	Reduction gear ratio	-
f	Flapping frequency	Hz
U_∞	Free stream velocity	ms^{-1}
k	Stiffness of the membrane sheet	-
S	Wing area	m^2
V	Applied voltage	volts
W	Weight	kg
c	Wing chord	m
t_w	Wing membrane thickness	mm
b	Wing semi span	mm
E	Elastic modulus	N/m^2
h	Camber height	mm
J	Advance ratio	-
L_{avg}	Lift average	N
D_{avg}	Drag average	N
C_{Lavg}	Lift coefficient avg	-
C_{Davg}	Drag coefficient avg	-
$\overline{c}$	Mean chord wing	m
$\bar{x}$	Mean	-
e_i	error	-

R^2	Correlation coefficient	-
SD	Standard deviation	-
t	Time	s
$\underset{u}{\rightarrow}$	Velocity vector	m/s
u_g	Grid velocity	m/s
V	Control volume	m^3
$\underset{V}{\rightarrow}$	Velocity vector	-
x, y, z	Space coordinates	m
X	Variable value	-
Y	Dissipation coefficient	-
E_c	Relative error	-
Cp	Pressure coefficient	-
u	Local velocity	m/s
U	Dimensionless velocity	-

Greek Symbols

ρ	Air density	kg/m^3
Θ_f	Flapping angle	^{0}
Θ_w	Flapping axis	^{0}
Ξ	Specific stiffness	-
β	Eigen value	-
β_0	Constant coefficient	-
β_j	Linear interaction coefficient	-
β_{jj}	Quadratic interaction coefficient	-
β_{ij}	Second-order terms	-
ε_{aero}	Aerodynamic performance	-

υ	Circulation	-
σ_x	Standard deviation	-
$\sigma_{\bar{x}}$	Standard error	-
v	Kinematics viscosity	m^2s^{-1}

LIST OF ABBREVIATION

MAVs	Micro Air Vehicles
FW-MAV	Flapping wing Micro Air Vehicles
Re	Reynolds number
LAR	Low aspect ratio
ECS	Electronic control system
RSM	Response surface methodology
2D	Two-dimensional
3D	Three-dimensional
AoA	Angle of attack
CCD	Central Composite Design
MEMS	Micro Electro Mechanical System
PVDF	Polyvinylidene fluoride
IPMC	Ionic Polymer Metal Composite
PVD	Physical Vapour Deposition
MFC	Micro fibre composite
PVC	Poly Vinyl Chloride
LIPCA	Lightweight piezo composite actuator
LEV	leading edge vortex

PIV	Particle image velocimetry
FSI	Fluid structure interaction
ALE	Arbitrary Lagrange-Eulerian
DM	Dynamic mesh
CFD	Computational fluid dynamic
LES	Large-Eddy Simulations
UDF	User Define Function
SD	Spectral difference
GA	Genetic Algorithms
SQP	Sequential Quadratic Programming
DOE	Design of experiment
NBC	National Broadcasting Company
VTOL	Vertical take-off and landing
DC	Direct current
GUI	Graphical User Interface
CAD	Computer aided design
CNC	Computer numerical control
PWM	Pulse Width Modulation
RPS	Revolution persecond
ADC	Analog Digital Converter
ZI²C	Inter-Integrated Circuit
PIC	Peripheral Interface Controller
ICSP	In-Circuit Serial Programming
USART	Universal Asynchronous Receiver Transmitter
RPS	Rotation per second

PC	Personal computer
COM	Component object model
DAQ	Data Acquisition Board
LDA	Laser Doppler Anemometry
ANOVA	Analysis of variance
S-A	Spalart-Allmaras
SIMPLE	Semi-implicit pressure-linked equations
CM	Coarse mesh
FM	Fine mesh
LE	Leading edge
LEV	Leading edge vortex
TV	Trailing vortex
LEV	Leading edge vortex
LE	Leading edge
TV	Trailing vortex
TE	Trailing edge

KAJIAN EKSPERIMEN DAN BERANGKA TERHADAP PRESTASI KEANJALAN KULIT SAYAP BERKEPAK UNTUK APLIKASI PESAWAT TERBANG MIKRO

ABSTRAK

Pesawat terbang sayap berkepak mikro (FW-MAVs) adalah pesawat terbang sebesar tapak tangan yang boleh bergerak di dalam persekitaran tempat yang sempit, nisbah aspek yang rendah dan mempunyai keupayaan untuk terbang dalam persekitaran nombor Reynolds yang rendah. Mamalia terbang seperti kelawar dan tupai terbang berkongsi satu ciri yang unik yang membolehkan mereka untuk terbang dengan ketangkasan pergerakkan yang menakjubkan dan tidak dapat ditandingi oleh haiwan terbang lain yang sama saiz dengannya. Ciri-ciri unik yang membolehkan haiwan-haiwan ini mempunyai keupayaan terbang dengan fungsi sayap membran yang nipis dan anjal. Didalam kajian ini, ciri-ciri unik sayap membran yang anjal dikaitkan dengan mamalia terbang seperti kelawar dikaji berdasarkan prestasi aerodinamik. Matlamat utama kajian ini adalah untuk menggabungkan mekanisme yang terlibat yang didapati daripada mamalia terbang untuk menghasilkan prestasi aerodinamik yang lebih baik terhadap MAV. Sistem Kawalan Elektronik (ECS) telah diperkenalkan untuk mengawasi mekanisme sayap semasa mengepak dengan menjadikan sayap kelawar sebagai contoh kajian bagi pesawat terbang berkepak mikro (MAV). Selain itu, ujian aerodinamik telah dijalankan di ruang angin terbuka untuk menyiasat ciri-ciri aerodinamik, terutamanya fleksibiliti kulit sayap dan kesan kamber. Tambahan pula, pengoptimuman menggunakan kaedah permukaan sambutan (RSM) telah dijalankan untuk mengkaji hubungan interaktif setiap faktor dan mengoptimumkan prestasi aerodinamik. Di samping itu, simulasi tiga dimensi

juga telah dicapai pada sayap rata dan kamber menggunakan perisian FLUENT. UDFs telah ditulis untuk meniru gerakan harmonik sayap mengepak dan model jaringan yang dinamik telah digunakan. Prestasi aerodinamik berdasarkan pekali daya angkat dan seretan dikaji berdasarkan fungsi AoA, frekuensi, dan kelajuan. Parameter Nisbah termaju juga telah diguna pakai untuk mengkaji kesan aliran tak mantap untuk sayap fleksibel dan kamber. ECS menunjukkan kawalan yang lebih cekap dengan pengukuran yang lebih tepat. Tambahan pula, sistem biasa yang memerlukan prosedur penentu ukuran ulangan telah berjaya diatasi dengan menggunakan ECS. Ia telah mendapati bahawa kulit sayap paling fleksibel paling sesuai untuk keadaan tak mantap dengan nisbah awal yang rendah, manakala sayap kurangnya fleksibel sesuai untuk julat yang lebih tinggi. Tambahan pula, keputusan ujikaji menunjukkan bahawa sayap berbentuk kamber mempunyai daya angkat dan seret jauh lebih tinggi berbanding dengan kes sayap rata. Selain itu, hasil yang optimum untuk prestasi aerodinamik sayap mengepak dicirikan berdasarkan kamber optimum, halaju, dan frekuensi didapati masing-masing 15%, 4.29 m / s, dan 9 Hz. Keputusan berangka yang diperolehi menyamai dengan penemuan eksperimen. Keputusan berangka mengesahkan peningkatan prestasi aerodinamik dan sayap kamber mampu meningkatkan sebanyak 1.12 kali berbanding sayap rata. Siasatan ke atas pembentukan kekuatan vorteks membuktikan bahawa sayap yang mempunyai kamber yang lebih tinggi dapat menjana kekuatan LEV yang lebih tinggi, dengan syarat bentuk corak vortisiti adalah lebih padat, lebih rapat, dan lebih pekat.

EXPERIMENTAL AND NUMERICAL INVESTIGATIONS ON THE PERFORMANCE OF FLEXIBLE SKIN FLAPPING WING FOR MICRO AERIAL VEHICLE APPLICATION

ABSTRACT

Flapping-wing micro air vehicles are small, hand-held flying vehicles that can maneuver in a constrained space because of its lightweight, low aspect ratio, and ability to fly in low Reynolds number environment. Flying mammals such as bats, and flying squirrels share a unique feature that allows them to fly with amazing agility and maneuverability unmatched by other flying animals of the same size. The unique feature that allows these animals to have such fight capabilities is their thin and flexible membrane wings. In this work, the unique characteristic features of flexible membrane wings associated with flying mammals such as bats are investigated for their highly efficient aerodynamic abilities. The primary goal of this study is to incorporate the mechanism involved in these flying mammals for improved aerodynamic performance of MAV's. An Electronic Control System (ECS) was introduced to control a proper flapper wing mechanism to emulate the wing flapping of bats for the ongoing micro air vehicle (MAV) research. Besides, aerodynamic tests were carried out in an open-air wind chamber to investigate the aerodynamic characteristics, particularly the wing skin flexibility and camber effect. Furthermore, the optimization using response surface methodology (RSM) was carried out to investigate the interactive relationship of each factor and optimize the aerodynamic performance. In addition to this, three-dimensional numerical simulation was also accomplished on flat and camber wing using FLUENT software. UDFs were written to mimic the harmonic motion of the flapping wing and the

dynamic mesh model was utilized. The aerodynamic performance based on lift and drag coefficient were investigated as functions of AoA, frequency, and velocity. Advance ratio parameter was adopted to study the effects of unsteady flow for flexible and camber wing. The proposed ECS demonstrates efficient control and accurate measurement. Moreover, the tedious procedure involved in the repeated calibrations for the manual system was totally eliminated by ECS. It was found that the most flexible wing skin was best suited for unsteady state with low advance ratio, whereas the least flexible wing was preferred for higher ranges. Furthermore, the experimental results showed that the cambered wings have significantly higher lift and drag when compared to that observed in case of flat wings. Moreover, the optimum result for the aerodynamic performance of the flapping wing characterized based on optimum camber, velocity, and frequency was found to be 15%, 4.29 m/s, and 9 Hz respectively. The numerical results were in good agreement with the experimental findings. The numerical results confirmed the enhancement of aerodynamic performance and camber wing was able to increase by as much as 1.12 times when compared to the flat wing. Investigation on the formation of vortices as well as its strength revealed that a higher camber wing was able to generate a higher LEV strength, provided the shape of the vorticity pattern was more compact, more attached, and more concentrated.

CHAPTER I

INTRODUCTION

1.1 Micro Air Vehicles (MAVs)

Recent developments in Micro air vehicles (MAVs) technology has potentially revolutionized the field of spying and data acquistion in military as well as civilian applications. It can be used to undertake military reconnaissance, crowd control, traffic management, survivor search, risky indoor inspection and other similar difficult tasks. In general MAV can be classified as: Fix-wing MAV, which is used for high endurance outdoor mission, Rotary-Wing MAV, for short endurance outdoor missions with hover and Flapping-wing MAV that are suitable for indoor applications (Galiński and Żbikowski, 2007) . Eventhough MAVs are designed to operate under difficult circumstances, they have several limiations. The conventional fix and rotary MAV does not fare well at very low Reynolds number (low flight air speed < 10 m/s) in comparison to its performancy at higher Reynolds numbers (Hu et al., 2010 and Pornsin-sirirak et al., 2001). Due to its wing span and surface area, the fixed wing MAV's have lower agility in avoiding indoor obstacles, and Rotary Wing-MAV's are too noisy as well as suffer from efficiency effects of low Reynolds numbers (Galiński and Żbikowski, 2007 and Hu et al., 2010).

In contrast to fix and rotary MAVs, a flapping flight offers good mauneuverability and agility in confined spaces and can be considered as an alternative to the conventional MAV’s. Several studies have been carried out to understand aerodynamics associated with the flapping mechanisms. They have established that Flapping wings derive their lift from the flapping motion of the wing

in contrast to the conventional MAVs which utilize the forward airspeed of the aircraft (Hu et al., 2010, Ho et al., 2003, Mazaheri and Ebrahimi, 2010). As a consequence, it offers less reliance on forward airspeed to generate lift and therefore the amount of lift generated can be controlled by the wings beat motion. As shown in Figure 1.1, the Reynolds number for MAVs and insects is in the range of 100 - 10,000. Airfoil performance of fixed-wing decreases substantially deteriorates for the Reynolds number at this range. Review by Ho et al., (2003) and Shyy et al., (2010) provides excellent information on the advances in aerodynamic performance of flapping wing micro air vehicle (FW-MAV). The success of a flapping mechanism lies in its ability to facilitate all the degrees of freedom while emulating the actual biological wing although maintaining symmetry and wide angle of flapping. . It is indeed a challenge to develop a mechanism which can mimic the actual biological wing having all degrees of freedom as demonstrated by natural fliers. The light weight and low aspect ratio FW-MAV is designed to fly under low Reynolds number conditions which makes it easily susceptible to environmental airstreams. Therefore there is a need for an improved wing having excellent aerodynamic features which can achieve stable and successful flight at low Reynolds number.

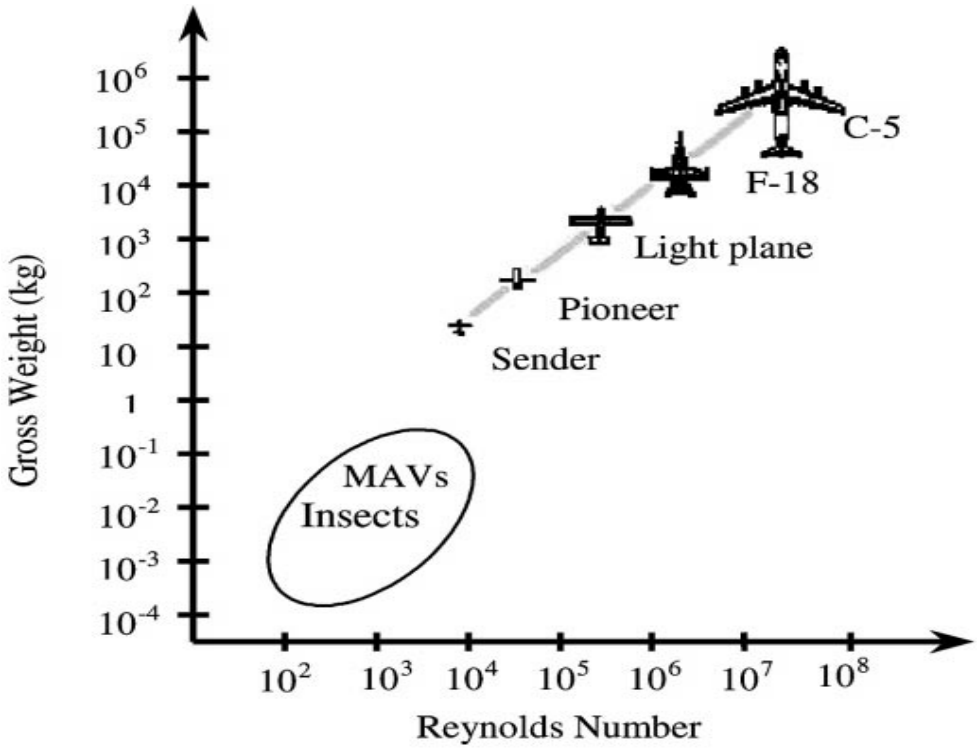

Figure 1.1: MAV flight regime compared to existing flight vehicles. Pornsin-sirirak et al., (2001)

1.2 Application of MAVs

Three types of popular MAV are developed in recent years; fix-wing, rotary wing and flapping wing. It is envisaged that MAVs can be used for direct reconnaissance for different environmental conditions. It is these environmental factors that impose various requirements on the design of the vehicle. MAVs can serve in many different applications and fulfil most of the trajectory requirements. Fortunately, different MAV configurations exhibit supplementary characteristics. It is therefore possible to tailor a certain requirement with a certain configuration. Different types of MAVs are word its characteristic features are shown in Figure 1.2.

Fix-wing	Rotary-wing	Flapping wing
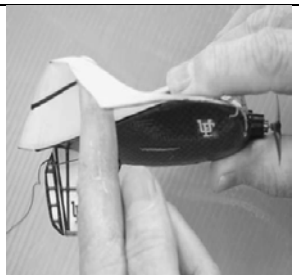		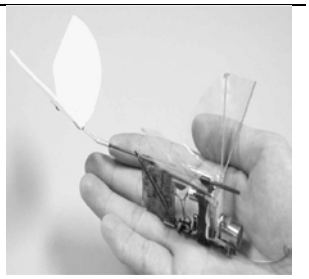
Albertani et al., (2007)	http://www.stanford.edu/mesicopter	Pornsin-sirirak et al., (2001)
		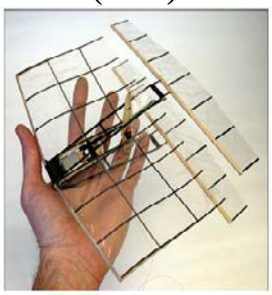
http://www.aerovironment.com	Barrientos et al., (2010)	Miao & Ho (2006)
		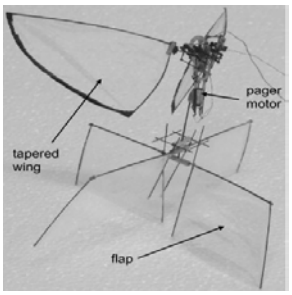
Galiński and Żbikowski, (2007)	Bohorquez et al., (2003)	Fenelon & Furukawa (2002)

Figure 1.2: Types of Fix-wing, rotary-wing and flapping wing MAVs

In general, MAVs are envisaged to perform any dirty, dull and dangerous reconnaissance missions in a direct neighbourhood of the operator. There are several typical missions reported by Galiński (2005), Galiński and Żbikowski (2007); such as outdoor NBC emergency reconnaissance, crowd control, suspect facilities, inspection of pollution, urban traffic management, search for survivors, pipeline inspection, and high risk indoor inspection. In performing NBC emergency

reconnaissance, an MAV serve the purpose of accessing hazardous situations such as an area with the presence of toxic gases where it will be difficult, even impossible, for a personnel to enter an perform tasks such as sample acquisitions.

In terms of law enforcement, MAVS serve the functions of crowd control through monitoring crowd behaviours during hostile situations where law enforcement officials cannot be directly involved. Another law enforcement uses of MAVs is through surveillance of suspect facilities where the presence of large flying objects will affect the behaviours of the suspect and thus affecting the case. MAVs also could serve green purposes by making regular pollution inspection convenient. Air samples can be collected without the attention of inspected companies and pollution carried by high and east winds can be collected by rotary MAV. Law enforcement or public officials can take the advantages of a short range or short endurance MAVs such as one that have VTOL capabilities for documentation of road accident documentation.

Surveillance system mounted on mobile platform such as MAVs can drastically simplify urban traffic management where mobile platforms make large number of systems obsolete. Search and rescue missions have recently enjoyed a number of successes thanks to MAVs. In cases like the 9/11 attack, rescuers can benefit flapping MAVs or even rotary MAV to search for survivors. In industry, large and complicated pipelines can be inspected with little preparation by using flapping wing MAV in place of robots. Similarly, flapping wings are useful in high risk indoor inspection such as inspecting laboratories filled with hazardous gasses. MAVs are particularly useful in simplifying the process which is rendered

complicated while using a number of fixed inspection systems. Table 1.1 and table 1.2 summarize the MAVs requirement and their applications.

Table 1.1: MAVs with mission specification and applications

Types of MAV	Mission requirement	Applications
Fixed-wing	long range and/or long duration missions in open space	Outdoor NBC emergency reconnaissance, Crowd control, and surveillance of suspect facilities
Rotary-wing	short endurance outdoors missions with hover	Regular pollution inspection, Road accident documentation and Urban traffic management
Flapping-wing	indoor missions	Search for survivors, Pipeline inspection and High risk indoors inspection.

Table 1.2: MAV characteristic

	Fast Flight			Hover		
Wing	Possibility	Efficiency	Manoeuvreability	Possibility	Efficiency	Manoeuvreability
Fix	yes	very good	very good	no	-	-
Rotary	yes	poor	moderate	yes	Poor	moderate
Flapping	no	-	-	Yes	very good	very good

1.3 Biologically of MAV designs

One motivation for the utilization of flexible membrane wings is to mimic the aeromechanics of natural flyers such as bats because MAVs operate in a similar flight parameter space as these biological flight systems, i.e. flying at low Re with low aspect ratio (LAR) wings. As the evolution of MAV design progresses, only a few studies were conducted recently to develop a model of the interplay of aerodynamic contributing to the better performance of flexible membrane flyers. The adaptive nature of the membrane wing may give MAVs the potential to mimic the extraordinary flight agility of bats. The morphing capability of the wing structure is the product of the interaction between fluid and structural capabilities. Shyy et al., (1999) discussed the development of computational techniques to assess the flow structure associated with LAR, low Reynolds wings and the generation of

optimization techniques for MAV wing shape. The structural deformation or dynamics of the flexible membrane greatly contributes to the aerodynamic forces over the wing and the wing performance. With inspiration derived from nature's flyers (refer to Figure 1.3.), MAV designers have focussed their attention towards flexible membrane wings to achieve improved agility and efficiency. Wings having thin and very flexible membranes are unique for flying and gliding mammals, such as bats, flying squirrels and sugar gliders. These animals exhibit extraordinary flight capabilities with respect to manoeuvring and agility that are not observed in other species of comparable size.

a) b)

Figure 1.3 a) Sugar glider by Galvao et al., (2006), b) the large degree of camber in the wing. The unique aerodynamic properties of a compliant-membrane wing are believed to play a significant role in the high degree of maneuverability exhibited by bats in flight by Song et al., (2008).

The rapid advancement in MAV design has driven the researches on flight of insects, birds and bats. Birds, in particular have been the centre of extensive study, and has shown relatively rigid wings with limited motion, while insects, which fly at

much lower Reynolds numbers, are typically characterized by rigid wings moving with a relatively simply articulated flapping motion (Galvao et al., 2006). On the other hand bat wings are made of quite flexible bones supporting very compliant and anisotropic wing membranes, and possess many more independently controllable joints than those of other animals. The mechanical characteristics of wings skin play an important role in determining the aerodynamic characteristics of the wing, and the motions at many hand joints are integrated to produce complex and functionally versatile dynamic wing conformations. It is observed that Bat wings are characterized by their sufficiently flexible bones supporting very compliant and anisotropic wing membranes; the unique features of bat wing as a promising candidate for MAV has been well established, as outlined by Swartz et al., (2007).

The founding researches on bat flight were summarized by Norberg (1976) who studied the kinematics, aerodynamics, and energetics of the long-eared bat *Plecotus auritus* in slow horizontal flight. A method, based on steady-state aerodynamic and momentum theories, is derived to calculate the lift and drag coefficients as averaged over the whole wing and the whole wing-stroke for horizontal flapping flight. The force coefficients, total mechanical power output, and mechanical and aerodynamic efficiencies are all plausible, demonstrating that the slow flapping flight of *Plecotus* is thus explicable by steady-state aerodynamics. The downstroke is the power stroke for the vertical upward forces and the upstroke for the horizontal forward forces. Bullen and McKenzie (2002) demonstrated scaling wing beat frequency and amplitude measured for 23 species of Australian bat. They found that wing beat frequency depends on bat mass and flight speed and wing beat amplitude depends on relationship between flight speed and wing area. The maximum value for wing beat frequency was observed to be about 4 to 13 Hz and

the wing beat amplitude ranged from 90 to 150 degrees. Pennycuick (1971) found that the bat's best gliding angle (about 6-8 degrees) is slightly better than that of the pigeon, but otherwise its low-speed performance is closely similar and bats are most probably more maneuverable than birds in low-speed flight, because of their greater control over the profile shape of the manus. There are thus no grounds for suggesting that the flight of bats is notably 'better' or ' worse' than that of birds. Each has an advantage in certain aspects of performance, but in most respects their abilities and flight efficiency are much the same. Aldridge (1986) demonstrated the kinematics and aerodynamics of the greater horseshoe bat, *Rhinolophus Ferrumequinum*, in horizontal flight. They showed that as flight speed increases there is a gradual change in the bat's wing beat kinematics, wing beat frequency decreasing and wing beat stroke plane angles increasing.

Norberg (1975) also described two manoeuvres in bats leading to loss of height: one such movement was by *Nyctalus noctula* rolling through 180 degree, and second one by *Otomops martiensseni* which showcased a series of sideslips. They found that these manoeuvres cause a rapid loss of height. They are initiated by pronation of one wing and supination of the other. After the roll, when the bat is in an upside down position, the lift force of the wings is directed downwards, causing a tight turn downwards (apparently for insect catching). During sideslip the body drag of the bat is increased. This reduces the total lift/drag ratio, thus steepening the equilibrium gliding angle. Aldridge (1991) described the kinematics, aerodynamics and energetic of vertical flight in *Rhinolophus ferrumequinum*. He found that during the downstroke the resultant force generated by the wings tends to accelerate the animal upwards and forwards. Towards the end of the downstroke the wings

generate negative thrust and, consequently, the animal accelerates backwards. When, during the upstroke, the wings are accelerated backwards (the 'flick') a significant thrust is generated. Total specific mechanical power required was approximately l l.92 W kg^{-1}, of which 84% is required during the downstroke. High-speed film analysis showed that the wing beat kinematics in *Glossophaga soricina* change gradually with increasing flight speed, indicating that there is no sudden gait change at any particular, critical, flight speed (Norberg and Winter, 2006). On the other hand, span ratio decreases significantly with increasing wing beat frequency. The Strouhal number a dimensionless parameter describing oscillating flow mechanisms and being a predictor of the unsteadiness of the flow, decreases with the flight speed.

1.4 Problem statement

Inspite several studies on MAV, the research on the aerodynamics of flapping-wing flight especially for inspired bat wing flapping MAV size is still in its nascent stage. Most of the earlier studies were directed towards understanding the biological perspectives of natural fliers and addressed fewer concerns about their practical applications in aerodynamics (Norberg, 1976, Bullen and McKenzie, 2002, Pennycuick, 1971, Aldridge, 1986, Norberg, 1975, Aldridge, 1991, and Norberg and Winter, 2006). In a study presented by Muijres et al., (2008), generating enough lift during hovering and slow forward flight was reported to be problematic in order to sustain flight in low Reynolds number regime. Nevertheless several species of small flying vertebrates have adapted to this low Reynolds number problem on account of their flexibility of wing skin membrane and cambering of wing shape (Galvao et al., 2006 and Song et al., 2008). Also, numerous studies on fix-wing MAV have focussed on flexibility and wing camber (Albertani et al., 2007, Stanford et al., 2008,

Song et al., 2008, and Null and Shkarayev, 2005). In the present work, the development of flaping wing based on compliance membrane skin and camber wing was investigated in order to study their effect on the aerodynamic performance based on lift and drag. The use of charateristic wing shape based on bat wing configuration is expected to enhance the aerodynamic performance during slow flapping flight. The work presented in this research provides the initial design guidelines for the practical design and implementation of future FW-MAV development.

1.5 Contribution of the present research

One of the biggest challenges that is faced during the study of this aerodynamic study of flexible skin flapping wing is the task of reproducing the proper biological wing and the flapping movement, a previous works have been done by other researchers in developing different types of wings along with their respective flapping systems for different applications, flapping mechanisms, and control system. To fill the need of providing more flexibility in measurements, an integrated electronic system is used to control and monitor the flapping frequency. In all of the previous works that have been done in this subject, researchers relied on external systems like an oscilloscope, optical sensor, and high speed camera to control the flapping frequency. The reason why these methods are used is because these methods allow the frequency of the given setting to be measured. Repeated calibration, large time consumption, and measurement inaccuracy at higher angle of attack (AoA) and velocity are some of the major drawbacks that is associated with the traditional ways of measuring the flapping frequency which necessitates an in-built electronic system to measure as well as control the flapping wing as it is more

convenient and effective. This brings to the development of a novel (ECS) to test a flapping wing system, which have been done by the present work.

Flying mammals such as bats, sugar gliders and flying squirrels share a unique feature that allows them to fly with amazing agility and maneuverability unmatched by other flying animals of the same size. The unique feature that allows these animals to have such fight capabilities is their thin and flexible membrane wings. This flight capability is so special that some engineers explored the potential of thin and flexible membrane wing for incorporation as lifting surfaces in MAV applications. In this work, the unique characteristic features of flexible membrane wings associated with flying mammals such as bats are investigated for their highly efficient aerodynamic abilities. The primary goal of this study is to incorporate the mechanism involved in these flying mammals for improved aerodynamic performance of MAV's. Earlier studies on flexible membrane wing MAV's have shown that that flexible membrane wings has the ability to achieve better agility and storage when compared to normal rigid wing MAV. Besides, flexible membrane wings can overcome the effects of gust wind and delay airfoil stall. Although several studies have been carried out, the basic thrust was in designing fixed-wing MAVs and only a few works dealt with the flexible skin and its effect on the aerodynamic performance of the MAV.

The development of flapping wing based on a compliance membrane skin with camber wing was investigated in detail in present work to study its aerodynamic performance. A comparison was made on three types of wing membrane with different flexibility along with several wings with different camber height to investigate the differences in their respective aerodynamic performance. In order to

estimate the number of experimental trials and the subsequent optimization of camber wing process, the design of experiment (DOE) technique is used.

Moreover, detailed flow field measurements quantifying the vortex formed on the flapping wing with respect to varying camber are still lacking. Therefore, numerical studies have been carried out to ascertain the experimental outcomes from flat and camber wing and provide a realistic comparison of the vortex developed.

1.6 Objective of the research

The present study is aimed to achieve the following objectives:

a. To develop an experimental setup for testing flapping wing system in order to study the effects on flexible wings, flapping mechanism, and develop an integrated electronic control system (ECS) to emulate the bat wing flapping mechanism in the micro air vehicle (MAV).

b. To carry out experimental investigation to study the effect of membrane thickness on the aerodynamic performance of the MAV model.

c. To study the effect of wing camber on the aerodynamic performance and carry out optimization study using design of experiment (DOE).

d. To perform three dimensional numerical simulation to study the flow behaviour on the flat and cambered wings, and validate with the experimental results.

1.7 Scope of the research

In this study the experimental setup based on flexible wings, flapping mechanism, and integrated electronic control system (ECS) was developed to

emulate the bat wing flapping for micro air vehicle (MAV) research. Three bat species having dimensions close to the design requirement of MAV, namely, *Mormopterus Planiceps, Nytophilus Geoffroyi, and Scotorepens Balstoni* were selected in accordance with the previous study by Bullen and McKenzie, (2002). The geometric details of wings and flight parameters were chosen based on their design. The experimental investigations focussed primarily on the effect of membrane flexibility on the aerodynamic performance of flexible latex flapping wings. Wings with membrane thickness 0.37mm, 0.28mm, and 0.13mm was selected which were almost of the same thickness of bat membrane skin reported by Swartz et al., (1996). These were represented as least flexible (A), flexible (B) and most flexible (C) respectively. The experiments were carried out in an air chamber having dimensions of 1.5m × 1.5m × 1.5m, subjected to wind velocities of up to 15 m/s. The time-averaged lift and drag as functions of the various parameters of flapping frequency, forward flight velocity, angle of attack (AoA) and advance ratio (J) were studied. Experiments were conducted, specifically focusing on the study of camber flapping wings for MAV application. Furthermore, detailed experimental investigation was carried out to evaluate the aerodynamic benefits of using camber wing in comparison with that of a flat wing study. The time averaged lift and drag generated from wings tested as a function of flapping frequency, free stream velocity, and the AoA was measured. A systematic experimental design based on the response surface methodology (RSM) was used to study the effects of design parameters on the aerodynamic efficiency (ε_{aero}) of the flapping wing. Additionally, the present study was extended to the quadratic model of RSM called Central Composite Design (CCD) to identify and optimize the flapping wing based on several factors like flapping frequency and free stream velocity. Lastly, the results of

lift and drag from experiment was compared with simulation results based on three different wings; flat wing, wing with 6% and 12% of camber. As reported by Busse et al., (2012), the maximum camber of 12% yielded the fast flight, and a mid-range camber of 6% yielded the slow flight. The characteristics of flow behaviour was studied and analysed to understand the camber effect on aerodynamic enhancement.

1.8 Thesis Outline

This thesis is organized in six chapters. Chapter one deals with introduction to Micro Air Vehicles (MAVs). The rationale for carrying out this research, its objectives and scope are presented in the introduction chapter. Chapter 2 provides the background of this study by reviewing relevant literature in this field. The effectiveness of flapping wing used for MAVs is discussed in this section. Moreover, a review of previous work dealing with aerodynamic enhancement and other parametric studies carried out to improve the performance characteristics of MAV is discussed. Chapter 3 explores the process of developing experimental model and set-up. Chapter 4 discusses about methodology of the experiment setup and simulation setup. Results, discussion and analysis of aerodynamic performance of experimental results and simulated results are presented and compared in chapter 5. Finally, conclusion and recommendation for future work is discussed in chapter 6.

CHAPTER 2

LITERATURE REVIEW

2.1 Overview

The aim of this chapter is to provide a thorough review of the current and past studies applicable to flapping wing and its application to MAVs. A brief review of development of flapping wing mechanism devices is initially discussed. Background of the aerodynamic design requirements relevant to present work is presented. Next the experimental studies on flapping wings are outlined, followed by numerical works discussing the dynamic mesh motion in particular are addressed. Finally, a survey of the published works on the optimization and application of the FW-MAV are also presented in detail.

2.2 Development of FW-MAV

Proper mimicking of the biological wing and its flapping is a challenging task in the study of aerodynamics of flexible skin flapping wings. Many researchers have developed different types of wings and flapping systems for diverse applications. An outline of the previous works on wing design, flapping mechanism, and control system is presented in this section. Pornsin-sirirak et al., (2000) developed a palm-sized ornithopter named “Microbat” with three different generations of prototype which is as seen in Figure 2.1. According to their report, the first generation prototype could fly only up to 9 seconds and it consisted of two 1 farad super capacitors that powered its flight. This lower flight duration was attributed to the fast discharge of the capacitor which failed to sustain the flight beyond 9 seconds. This drawback could be eliminated by using a rechargeable battery. Therefore they used a small 3-gram rechargeable Ni-Cad battery to power

the second type of prototype, which resulted in flight performance the first prototype, lasting about 22 seconds. Their last prototype had the ability to turn left or right and pitch up and down and was radio controlled. Pornsin-sirirak et al., (2001) reported the first Micro Electro Mechanical System (MEMS) based wing technology. They utilized titanium-alloy metal (Ti-6Al-4V) and poly-monochloro-para-xylylene (parylene-C) for constructing the wing frame. MEM facilitates development of a wing with minimum weight, and better repeatability, size control. They constructed a lightweight, palm-sized flapping-wing micro aerial vehicle (MAVs) with super capacitor-powered and battery-powered transmission systems. This MAV demonstrated a remarkable fight duration ranging from 5 to 18 s.

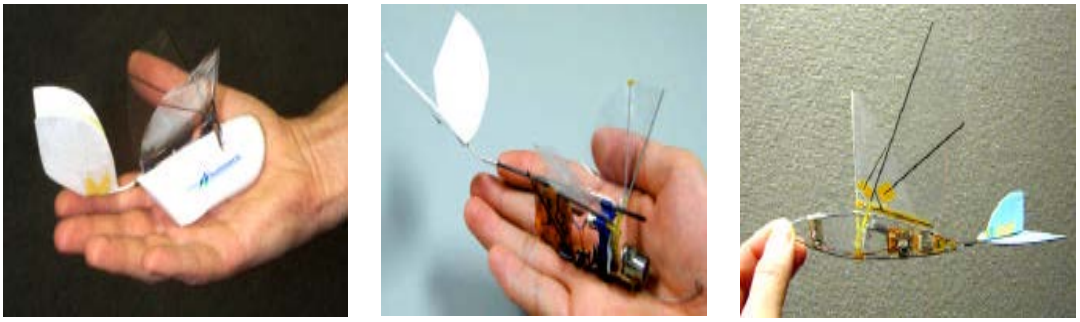

a)super capacitor-powered prototype (1 st generation)

b) battery-powered prototype (2 nd Generation)

c) battery-powered prototype with a radio control system (3 rd generation)

Figure 2.1: Three generation of Microbat prototypes developed by Pornsin-sirirak et al., (2000).

Pornsin-sirirak et al., (2002) further improved the aerodynamic performance by developing a flow control mimicking a wafer-sized parylene check-valved skin which facilitated micro adaptive flow control using MEMS wings. This regulated the pressure during both the downstroke and upstroke by distributing the actuators on

the wings and controlling the air movement below and upper wing skin through the vent holes as illustrated in Figure 2.2 a).

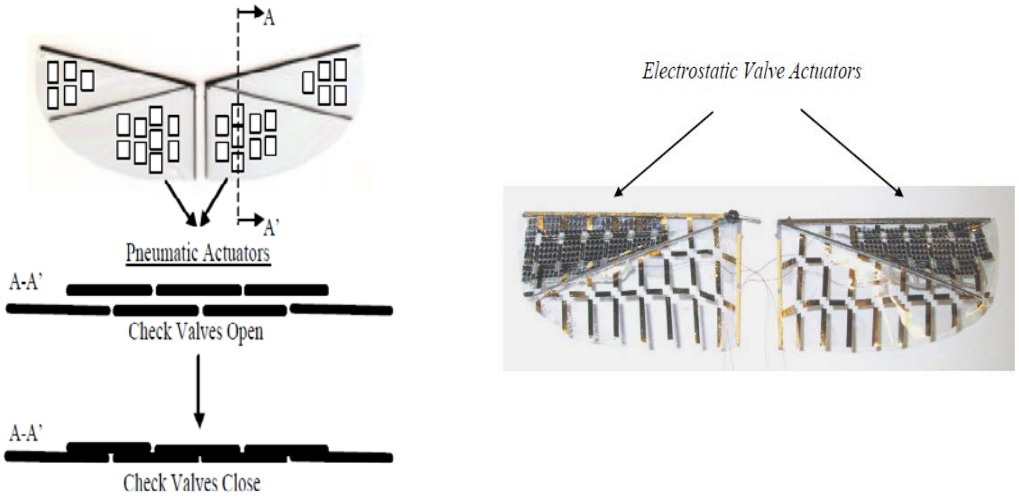

a) Passive valve actuator

b) Active valve actuator

Figure 2.2: a) Passive by Pornsin-sirirak et al., (2002) and b) active by Liger et al., (2002) adaptive of flow control actuator intended onto MEMs wing.

Liger et al., (2002) improved the functionality of wafer-sized parylene skins by integrating it with electrostatic valves that are employed on ornithopter wings for active adaptive airflow control using MEMS technology. Distributing electrostatic valves has its advantages as it helps control the pressure distribution on the wings during flapping as shown in Figure 2.2b. Yang et al., (2007) study a smart wing with PVDF–parylene composite skin by MEMs process and a four-bar linkage transmission system with variable phase lags of the flapping wings. The signals from the PVDF film and the load-cell are acquired simultaneously and the curves are quite similar. This result demonstrates that the smart PVDF skin has the promising capability to monitor aerodynamic information of flapping in the future. In the wind-tunnel tests, the collected data has a phase lag between the PVDF and load-cell

curves due to the design of asymmetric flapping movement. By a superimposing method, the “pseudo” PVDF curve has higher similarity to the lift signals. The smart PVDF–parylene composite wing and the superimposing method can help to design a micro MAV with ideal aerodynamic characteristic by changing the phase lag between the two flapping wings through fine tuning of the mechanism linkages.

The micro air vehicle designed by Jones et al., (2004) used flapping wings for its flight. The symmetric flapping wing pair provides a mechanically and aerodynamically balanced platform. The wings flapped in counter phase, and generated ground effect and stall suppression effect which increased the flight efficiency. The configuration developed is shown in Figure 2.3.

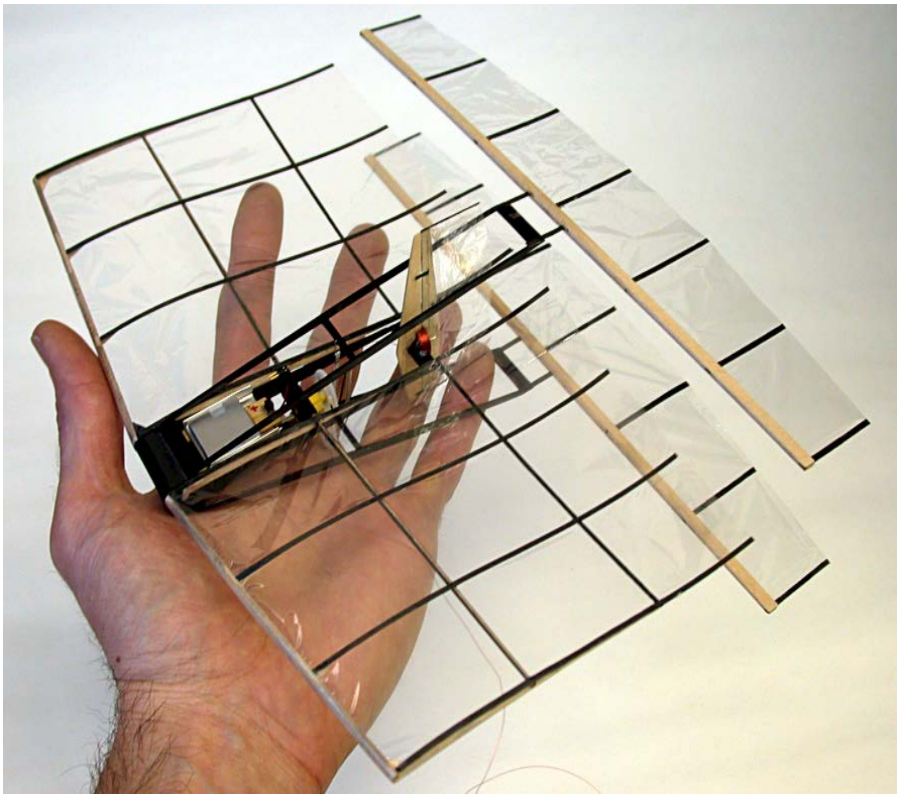

Figure 2.3: Propelled by a pair of wing symmetry produced by Jones et al., (2004)

The flapping wings developed by Lee et al., (2006) employed Ionic Polymer Metal Composite (IPMC) devices actuated by a linkage system. Investigations were carried out to test the flapping performance of these devices. These experiments demonstrated the identification of the best combination of cat ion and solvent of IPMC that accounts for least solvent loss and increase in actuation force. It was established from these tests that IPMC having solvent made of heavy water had higher operation time. They also showed that higher actuation force could be generated on shorter and thicker IPMC's; however their actuation displacement was much lower. Using the Physical Vapour Deposition (PVD) process, gold was sputtered on both surfaces of the cast IPMCs which improved the surface conductivity and minimized solvent evaporation due to electrically heated electrodes. A rack-and-pinion type hinge provided the necessary amplification required for the short IPMC's having small actuation displacement for the large flapping motion. The insect wing attached to the IPMC flapping mechanism for its flapping test used IPMC having thickness of 800μm. This could produce a flapping frequency of about 0.5~15Hz and flapping angles around 10°~85° on application of 3~4V.

Kim and Han (2005) investigated the aerodynamic characteristics of a smart flapping wing made up of macro-fiber composites (MFC) actuator related to birds and ornithopters. The membrane was made of PVC. The wing camber could be replaced using the MFC actuator to enhance the aerodynamic performance of the wing. Lin et al., (2006) developed flexible wings with carbon fibre frame and PVC plastic film membrane to simulate the flapping motion of birds by means of four-bar linkage mechanism. Mcintosh et al., (2006) devised a novel mechanism of a hovering MAV to mimic the wing motion of hummingbird and hovering insects. The

mechanism used a single actuator, but each wing could rotate about two orthogonal axes. The wings were made of carbon fiber frame and nylon fabric membrane. Nguyen et al., (2009) and (2010) presented the design of a motor-driven flapping-wing system which emulated the beetle (*Allomyrinadichotoma*), in terms of dimension, flapping frequency, and wing kinematics. Carbon fiber was used as wing frame and kapton film as membrane. Hu et al., (2010) studied the aerodynamic benefits of flexible membrane wings for the development of FW-MAV. A comparative study was carried out between the time-averaged lift and drag coefficient for the rigid wing and two flexible membrane wings made of nylon and latex materials having different skin flexibility.

Big challenge to produce movement forms a robust mechanism and it is not easy to be designed based on mechanical characteristics. To overcome these problems multifarious wing flap mechanism was developed and designed by previous researchers based on inspiration and ideas acquired from the winged animal movement mechanism. With a basic four-bar linkage mechanism, researchers have tackled this issue in a variety of fashions. Baskar and Muniappan, (2003) compared three flapping mechanisms namely sliding link, movable hinge, and fixed hinge, and found that the fixed hinge mechanism was free from unsymmetrical flapping and strut movement. In a study on the energetics of FW-MAV, Madangopal et al., (2005) used single-crank mechanism with springs to duplicate the flying of insects; similar mechanism without springs was used by Lin et al., (2006). There are some critical problems in developing mechanical design of flapping wing system. Basically, wing flapping should create convenient angles and allow the wings current rotation to mobilize up and down stroke. Besides, identifying suitable flap actuators is another

challenge in the design of biomimetic flapping devices. There is a need for creative ideas in order to move innovative system. This is because the current pneumatic motor driven system is not at all suitable for small robots or micro size flapping robots owing to its large payload and complexity of the system involved. Moreover, the flapping system actuator produces only limited actuation displacement. The limited actuator displacement can be easily overcome by combining a four bar linkage mechanism similar to the one introduced by Syaifuddin et al., (2005). However, this 4 bar mechanism failed to produce the requisite amount of flapping amplitude under bending motion.

The lack of flapping symmetry encountered in the single-crank four-bar system was rectified by the use of double crank in series, as proposed by Mcintosh et al., (2006). However, Conn et al., (2007) demonstrated that the flapping angle could be improved further by using double crank in parallel. Employing a slider with single crank was another way of maintaining flapping symmetry, and this technique was simpler compared to the use of double crank. Recently, Fenelon and Furukawa, (2010) have proposed a modified slider-crank mechanism, in which a rotary actuator was employed for the spherical joint, in order to enhance the degrees of freedom. As remarkable contribution to MAV research, Wood, (2007,2008), Finio and Wood, (2010), Sreetharan and Wood, (2010) and Sitti, (2003) developed and analysed four-bar linkage flapping wing system inspired by the thoracic mechanism of insects. A deviation from the basic four bar linkage was the use of Scotch Yoke linkage mechanism, as proposed by Galinski and Zbikowski, (2005) and Nguyen et al., (2010 and 2011). Table 2.1 summarize the transmissions system and flapping frequency measurement.

Table 2.1: Flapping mechanism based on experimental setup

Authors	Transmission design	Flapping control
Pornsin-sirirak et al., (2000)	Fourbar linkage	-
Pornsin-sirirak et al., (2001)	Fourbar linkage	-
Pornsin-sirirak et al., (2002)	Fourbar linkage	-
Liger et al., (2002)	Fourbar linkage	-
Yang et al., (2007)	Fourbar linkage	Voltage control
Jones et al., (2004)	Actuator	Not given
Lee et al., (2006)	Actuator	Voltage control
Kim and Han, (2005)	Fourbar linkage	Voltage control
Lin et al., (2006)	Fourbar linkage	Oscilloscope
Mcintosh et al., (2006)	Fourbar linkage (biaxial rotation)	Encoder
Nguyen et al., (2009) and (2010)	Fourbar linkage with Scotch Yoke	High speed camera
Hu et al., (2010)	Fourbar linkage	Voltage control
Baskar and Muniappan, (2003)	Slider mechanism	Opto-coupler sensor and oscilloscope
Madangopal et al., (2005)	Single-crank mechanism with springs	-
Syaifuddin et al., (2005)	Fourbar linkage couple with actuator	High speed camera
Conn et al., (2007)	Parallel crank rocker	High speed camera
Fenelon and Furukawa, (2010)	Slider-crank mechanism, in which a rotary actuator	Voltage control
Wood, (2007,2008)	Fourbar linkage	Voltage control
Finio and Wood, (2010)	Actuator	Retroreflective markers
Sreetharan and Wood, (2010)	Actuator	High speed camera
Sitti, (2003)	Piezo electrically Actuated Four-Bar Mechanism	Optical microscope
Galinski and Zbikowski, (2005)	Fourbar linkage with Scotch Yoke	High speed camera

2.3 Aerodynamic mechanism of flapping wing

2.3.1 Wagner Effect

As the wing begins its flight motion under high angle of attack, the airflow vortices do not immediately achieve their steady state value. This delay is due to the combination of two phenomena discussed by Sane, (2003). Firstly the fluid is inviscid, meaning it has no viscosity and therefore represents non-viscous behaviour at stagnation point and therefore it requires certain time duration to establish the

Kutta condition. Second, during the process the vorticity is generated and again shed at the trailing edge, while this shed vorticity forms a starting vortex. The velocity field near the wing, which is induced by the shed vorticity at the trailing edge counteracts to the bounding of the vortex to the wing. Only when the starting vortex has moved enough far away of the trailing edge, the moved wing gets its maximum circulation. This phenomenon involving slow development of circulation was first proposed by Wagner in 1925, hence the name Wagner effect is illustrated in Figure 2.4. Unlike the other unsteady mechanisms, this effect is not as strong. Particularly at Reynolds numbers (10^2 – 10^4), which are typically for small birds or insects it can be neglected for flapping wings.

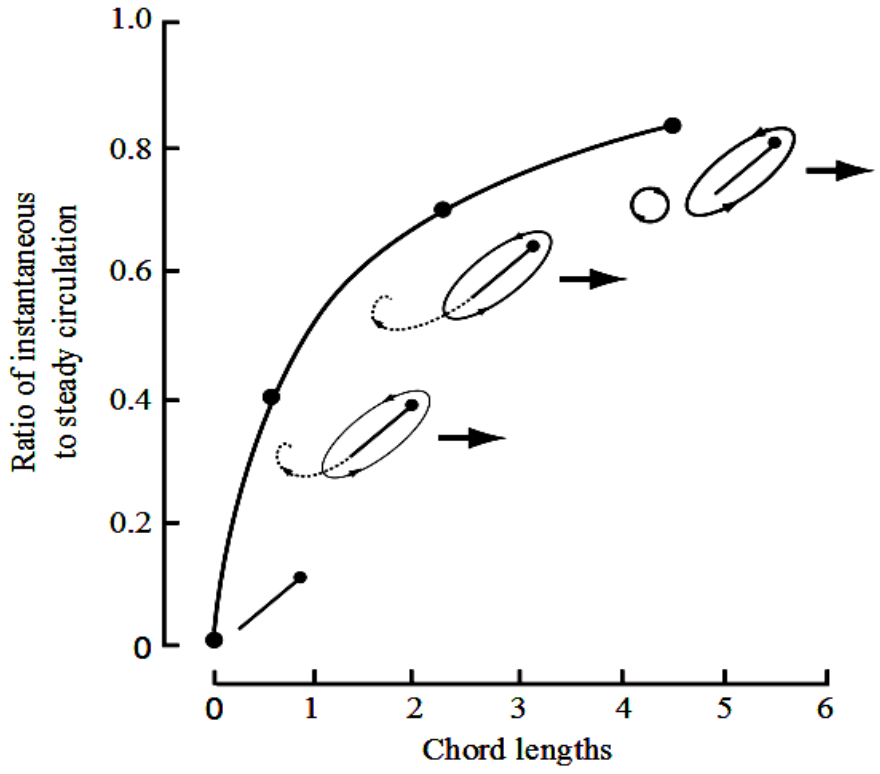

Figure 2.4: Wagner effect. The ratio of instantaneous to steady circulation (*y*-axis) grows as the trailing edge vortex moves away from the airfoil (inset), and its influence on the circulation around the airfoil diminishes with distance (*x*-axis) by Sane, (2003).